Mechanical Design of Light Engine for 3D printer

Nicolas Blondon

School of Engineering

Internship Project

August 2023

Responsible
Prof. Christophe Moser
EPFL / LAPD

Supervisors
Jorge Madrid Wolff
Maria Isabel Alvarez Castaño
Felix Wechsler
EPFL / LAPD

Table of contents

1 Introduction

Novel 3D printing technologies have the potential to revolutionize manufacturing and supply chains, as well as open new fields of study, such as tissue engineering. These modern techniques rely on accurate light display. In tomographic volumetric printing, a technology developed at EPFL's Laboratory of Applied Photonics Devices (LAPD), light from multiple lasers is projected onto a Digital Micromirror Device (DMD). The accurate alignment of this device is crucial for successful 3D printing.

2 Background

2.1 Tomographic Volumetric 3D printing

Tomographic volumetric 3D printing [1], or tomographic volumetric additive manufacturing (Tomographic VAM), uses a laser-based procedure to cure resin through a process called photopolymerization. The laser is focused on the surface of a DMD, which can be configured to show patterns. These patterns are reflected onto a vial of resin, which is then solidified into an object. To reach the desired object's specifications, the vial rotates at a set speed, implying that the patterns reflected from the DMD must also change.

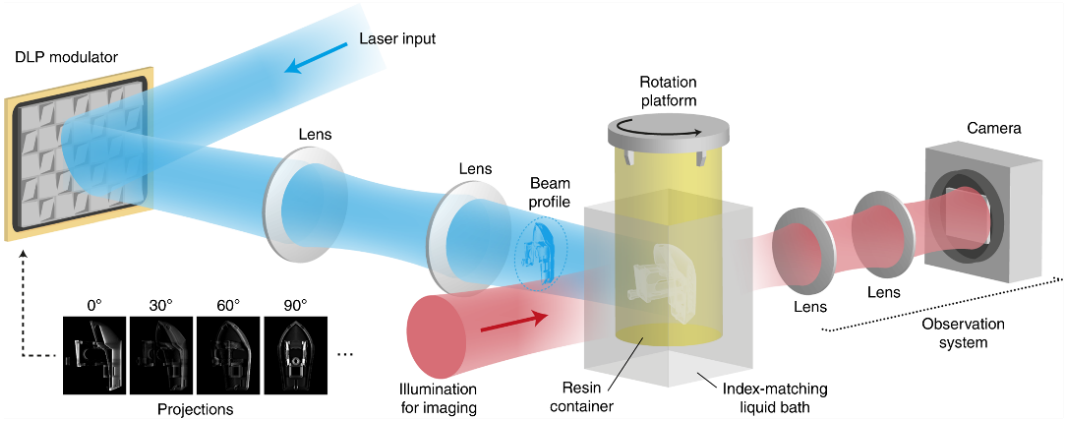

Figure 1: Diagram of a Tomographic VAM printer

Tomographic volumetric 3D printing is quite different from layer-by-layer 3D printing techniques. It is much faster than most additive manufacturing technologies, such as Fused Deposition Modeling (FDM) or Stereolithography (SLA). FDM printing is the most widely used type of 3D printing at consumer level. These machines work by heating and melting a thermoplastic filament into a layer of an object. This process is repeated until the object is completed. SLA printers resemble Tomographic VAM printers in that they also use photopoylmerization to print objects. However, they can only print a single layer at a time, resembling FDMs. Compared to FDM, they have much better resolution and quality, as well as faster printing speed, but at the price of a higher cost. SLA is mostly used by professionals. Both of these methods are layer-by-layer processes and can be time-consuming. On the other hand, Tomographic VAM works much faster since the object is printed all at once.

2.2 Diffraction grating

A diffraction grating is an optical device designed to disperse light into its component colors or wavelengths by exploiting the phenomenon of diffraction. It consists of a surface with a series of closely spaced, parallel lines or slits that interact with incoming light waves. When light passes through or reflects off a diffraction grating, it spreads out into a spectrum of colors due to interference patterns created by the interaction between the individual slits or lines and the incident light waves. This dispersion of light is the fundamental principle behind the operation of diffraction gratings.

A Digital Micromirror Device (DMD) is an instrument composed of a an array of tiny square mirrors, or pixels, that can be individually tilted, about an axis connecting two opposing corners of a single pixel. This allows the user to control the direction of light. By selectively reflecting or transmitting light from specific regions of the diffraction pattern created by the grating, DMDs can control which wavelengths or colors are displayed or detected.

Figure 2: The DMD with the corresponding electronic board

The light arriving onto the DMD is called incident light. When white light, or a laser beam is incident on the DMD, it encounters the closely spaced slits or lines separating each mirror. Each line on the DMD acts as a point source of secondary waves. These secondary waves spread out from each slit, and they interfere constructively or destructively with each other, depending on their relative phase differences. This interference creates a pattern of bright and dark regions. The angles at which the light waves emerge from the DMD depend on their wavelength and the spacing between the slits, or size of the mirrors. This angle is determined by the grating equation.

$$n \cdot \lambda = d \cdot \sin(\beta)$$

Where n is the order of diffraction (an integer), λ is the wavelength of light, d is the spacing between the grating lines or slits, β is the angle of diffraction.

The different colors (wavelengths) of light are dispersed at different angles because of this relationship. This dispersion results in a spectrum of colors being separated spatially. If the incident light is only composed of

a single wavelength, the diffracted light will also be submitted to the diffraction effect of the grating. The reflected light will accumulate into diffraction orders, which are explained further into this paper.

In essence, DMDs offer a versatile way to manipulate and control light spectra in various applications, including spectroscopy, wavelength-selective imaging, and projection systems. They allow for precise control over the diffracted light patterns and enable the creation of complex optical devices with high spectral resolution and versatility.

Additionally, depending on the incident angle, diffraction orders of differing intensity may appear. The two primary diffraction orders are the following :

- **The Zeroth order:** The zeroth order corresponds to the undeviated or central beam. This is the primary, unaltered direction of the incident light, and it is often represented as "$m = 0$" in diffraction equations. In the context of a diffraction grating, the zeroth order corresponds to the central maximum in the resulting diffraction pattern. It is also the order carrying the most energy. An ideal situation would be to only visualize the zeroth order, as to not experience a loss of energy.
- **Higher orders:** Higher diffraction orders correspond to the beams that are deflected at various angles away from the zeroth order. These are represented as "$m = \pm 1, \pm 2, \pm 3, ...$" and so on. Each higher order corresponds to a specific angular deviation from the central beam, and they form a series of angularly spaced beams. In the case of the DMD, these orders appear in a square formation and each additional copy is a loss of energy.

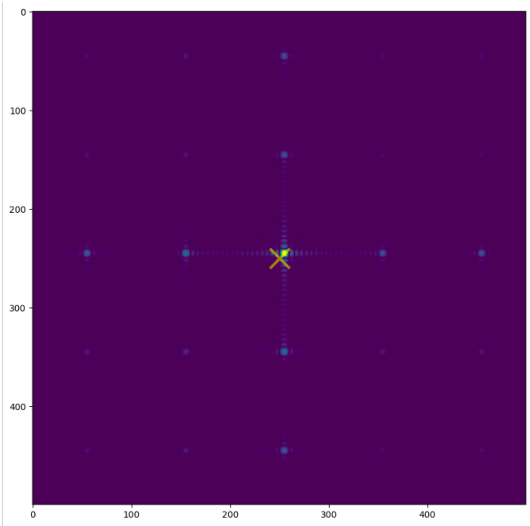

Figure 3: Zeroth order of diffraction

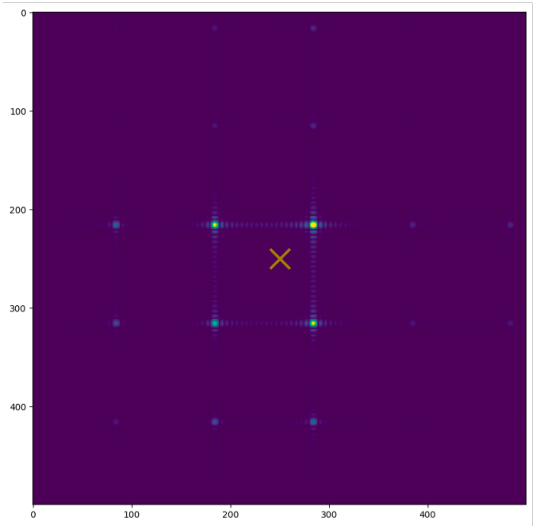

Figure 4: Higher orders of diffraction

To put differently, the zeroth order leads to the maximal efficiency, as there is almost no energy dissipation. Nevertheless, the experiments conducted will illustrate that attaining the maximum efficiency while adhering to the other mechanical and physical constraints is a complex endeavor. Further details of the experiments will be described later in the report.

2.3 Changing wavelengths

At the commencement of this internship, the laboratory's printer was exclusively compatible with laser sources emitting at a wavelength of 405 micrometers. The primary objective of this project was to introduce versatility by accommodating various wavelengths.

Nevertheless, the introduction of multiple wavelengths presents complications. Each distinct wavelength necessitates meticulous calibration of the DMD due to the grating equation. Thus, the DMD must have multiple degrees of freedom to reach the calibrated position, insuring maximum efficiency.

2.4 A game of angles

The most significant challenge lies in supporting the DMD such as the incident angle α diffracts into the zeroth order of diffraction, all while assuring that the reflected angle β stays parallel to the breadboard's surface and is oriented in the right direction.

This can be calculated. All angles used in this section are in radians. The conversions between radians and degrees are:

$$\theta_{radian} = \frac{\theta_{degree}}{180} \cdot \pi \qquad \theta_{degree} = \frac{\theta_{radian}}{\pi} \cdot 180$$

Where θ_{degree} and θ_{radian} are corresponding angles in degrees and radians, respectively.

To better understand the angles at play, Fig.5 presents a schematic of the DMD's screen.

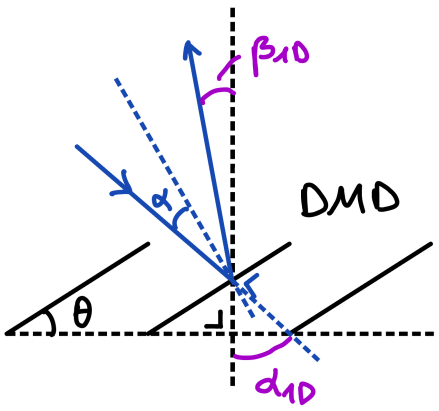

Figure 5: Schematic of the useful angles

To determine the incident angle (in $\hat{x}$, $\hat{y}$ and $\hat{z}$) with respect to the horizontal axis the reflected beam must follow, called $\vec{n}$, which only has an $\hat{x}$ coordinate, we must use geometry. $\hat{x}$ and $\hat{y}$ are unit vectors, $\hat{x}$ points into the optimal reflected beam position, $\hat{y}$ is aimed horizontally across the DMD's screen and $\hat{z}$ is oriented vertically. The Python script to optimize for efficiency (more information in the section 2.5) has the incident angle according to an individual pixel's normal. Evaluating this angle with respect to $\vec{n}$ allows for better

comprehension and implementation of said angle. Let α be the incident angle according to an individual pixel's normal, α_{1D} be the corresponding angle with respect to $\vec{n}$. α_{1D} is the same in both the xy and xz planes since the DMD's pixels are square-shaped. A simple geometric equation can be found to transform α into α_{1D}:

$$\alpha_{1D} = \arctan\left(\frac{\tan(\alpha)}{\sqrt{2}}\right)$$

θ is an intrinsic propriety of the DMD and has a value of 12° in this setup. (0.20944 radians). θ_{1D} can then be calculated,

$$\theta_{1D} = \arctan\left(\frac{\tan(\theta)}{\sqrt{2}}\right)$$

$$\theta_{1D} = 0.149 \text{ radians (or } 8.548 \text{ degrees)}$$

We can also calculate the reflected angle β (and β_{1D}, with the same references as the incident angles):

Using geometry,

$$\beta_{1D} = 2\theta_{1D} - \alpha_{1D}$$

and

$$\beta = \arctan\left(\frac{\tan(\beta_{1D})}{\sqrt{2}}\right)$$

After the first tests, showing inconclusive results, modifications were made to the system and the Python script to gain efficiency and precise positioning.

Mathematically,

$$\alpha_{1Dnew} = \alpha_{1D} - \beta_{1D}$$

This small change was crucial in reaching a suitable outcome.

$$\alpha_{1Dnew} > \alpha_{1D} \qquad \text{because} \qquad \beta_{1D} < 0$$

These equations imply that the incident angle is displaced into a position where the reflected angle is 0° with respect to $\vec{n}$. The angle between the laser's output and the DMD's screen must be widened, in both xy and xz planes.

Before using the angles found in this section, it is recommended to transform them into degrees.

2.5 Python scripts

Most of the mathematical equations were calculated using Python scripts. The first code used in this project was written by Sébastien Popoff [2], to determine optimal incident angles. Using the information received, another program was written to implement, transform and calculate the necessary values to build and calibrate the setup. This second code had to be modified to reach the final outcome.

Full versions of these programs can be found on the authors' GitHub pages [3] [4].

2.6 How the setup works

A 50 milliwatt laser is focused into a square optical fiber of 200 micrometers of width, which is then attached to the end of the laser arm, shown in Fig.6. The resultant beam is then passed through an aspherical lens of 2 millimeters of focal length, and two cylindrical lenses of respectively, 250 and 300 millimeters of focal distance. At this point, the beam reaches the screen of the DMD. It is then diffracted horizontally into an aperture, or iris.

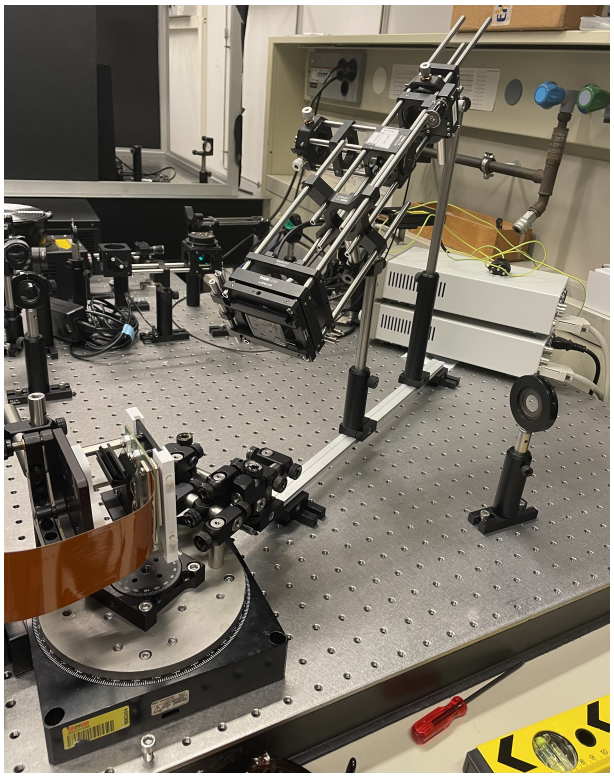

Figure 6: Final prototype and setup

3 Objectives and Scope

The objective of this research project was to develop, design and test a new support for the DMD in EPFL's LAPD's 3D printer. The updated support enables the user to easily calibrate and use the printer with lasers of different wavelengths. These changes were also necessary since the DMD used in this project is a newer version of the device currently in the printer. Thus, the dimensions of both pieces of hardware are not the same and the supporting mount had to be modified.

To reach this goal, multiple methods and techniques were employed, such as 3D modelling, 3D printing and dynamic testing. The software used for the design phase was CATIA v5. The prototypes were 3D printed with a SLA printer from FormLabs. The prototype was built using hardware and parts from ThorLabs, an american optical equipment company.

4 Methodology

This project was divided into three distinct phases. The first phase involved the design process, during which CAD (Computer-Aided Design) files were created and modified to meet the specified constraints. Then, during the prototyping phase, a mock-up was built to test the design that had been chosen. The final version was then ordered and built. Lastly, the testing phase began and final adjustments and corrections were made.

5 Design Phase

During the inspection of the old support, shown in Fig.7, multiple problematic points were raised. There was only one degree of freedom and the connection to the breadboard, or surface of the optomechanical table, was not centered around the DMD's screen. This is important since the angles required for the correct calibration are calculated about the screen.

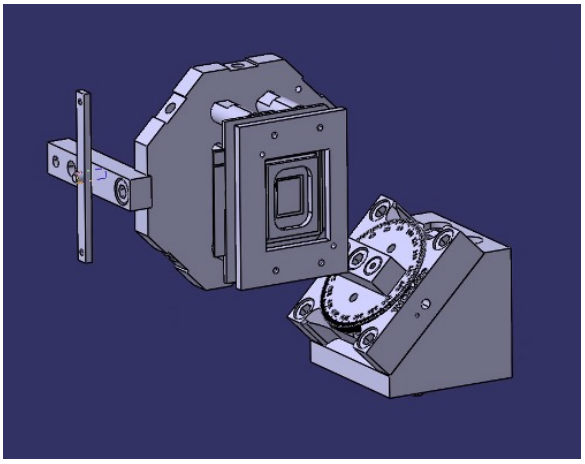

Figure 7: CAD of the old support

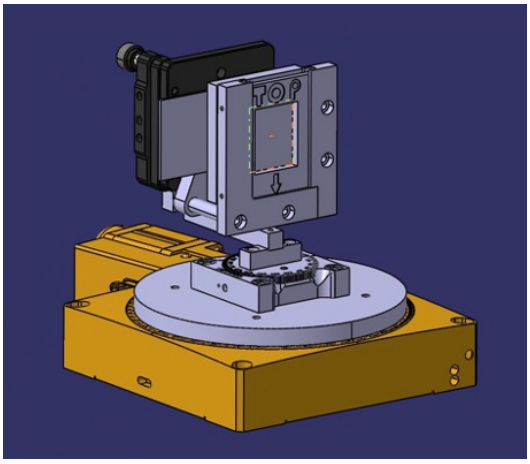

Figure 8: CAD of the new design

The design of the new support is mostly based off of the old version, as exhibited in Fig.8. However, all the

parts are completely new, nothing was able to be recycled. The concept behind the design is based around two rotation stages, one on top of the other. When the bottom one rotates, the upper stage will move in the opposite direction, assuring that the DMD stays in the same position during any motion. To ensure that the top stage can not change position, a connection is made between the breadboard and the stage, preventing any rotation. This beam does not interact with the bottom stage, allowing all movement of the laser arm connected to the lower platform.

The laser arm is composed of multiple parts from ThorLabs, whose functions are to hold the optical fiber and the lenses, necessary for the correct alignment of the beam, at the correct distance.

The parts connecting the DMD to the upper rotation stage allow for small rotations (± 2 degrees in $\hat{x}$ and $\hat{y}$ directions). However, this rotation proved insufficient, mostly in the xz plane.

6 Prototyping Phase

The support's parts were 3D printed using the SLA printer (from FormLabs) that was available in the laboratory. However, the printer's precision did not meet the desired quality standards, as outlined in Fig.9. After tapping threads in the plastic parts, the support was assembled with screws (M4 and M6). This step was important to verify the compatibility of the DMD and the support. At this point in time, concerns were raised about the stability of the mount. These worries were pushed aside with the certainty that the plastic material was the cause, and once the final version was ordered, these problems would not persist. At this point in time, the final product was intended to be manufactured in aluminium, ensuring a rigid support. The final prototype would be 3D printed in a workshop on EPFL's campus (Atelier de Fabrication Additive, AFA), as shown in Fig.10. While there were still doubts about the rigidity and stability these components would provide, testing and using them quickly dispelled these uncertainties.

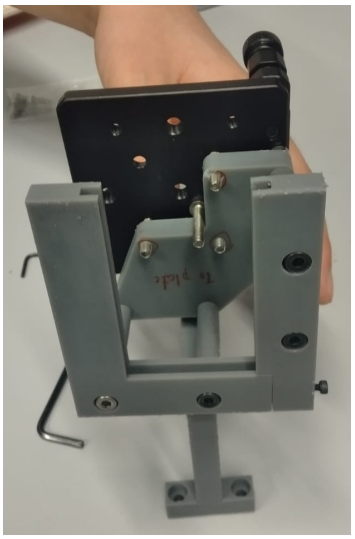

Figure 9: First 3D printed prototype

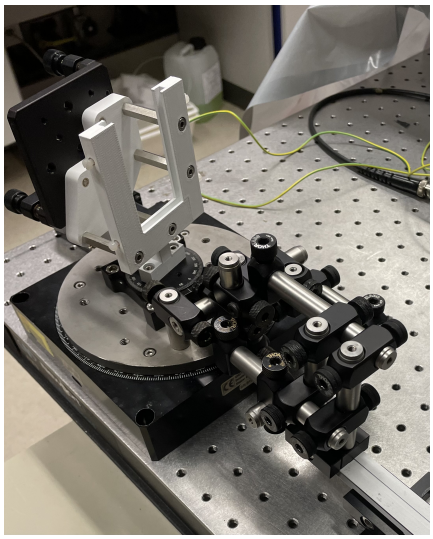

Figure 10: Final prototype, 3D printed

The next part of this project was dedicated to the construction of the connection between the bottom rotation stage and the laser arm.

Multiple versions were built, gradually becoming less and less bulky, to not block the laser beam's path, while conserving sufficient rigidity to ensure against the creation of undesired movement. This guarantees that the motion of the laser arm will only be influenced by the rotation stage, keeping the correct alignment of the laser.

Subsequently, the laser had to be aligned through the 3 lenses composing the laser arm. This procedure was time consuming as each lens has to be placed precisely on the arm, creating a beam of correct size and resolution. The arm is built around a rail system from ThorLabs, to keep the lenses centered and to facilitate the alignment process. Fig.11 shows the laser arm during the alignment operation.

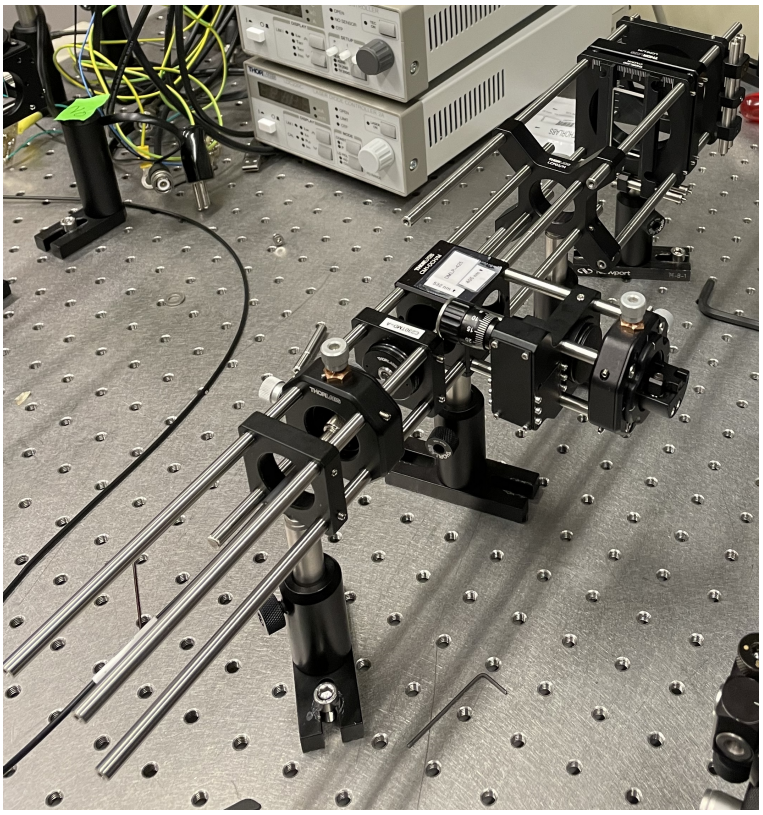

Figure 11: Laser arm during the alignment process

Alternatively, the lower rotation stage was taken from another student's Master Project. Michael Biselx worked on a small app for running reflectance measurements on a sample, using the NI USB-6002 Data Acquisition (DAQ) device Newport ESP301 Motion Controller + URS150BPP. Using his work as a starting platform, the program he wrote was adapted for our optomechanical setup [5] (The NI USB-6002 Data Acquisition (DAQ) was not used in the system).

7 Testing Phase

One of the goals of the project is to optimize the efficiency of the DMD's diffraction. Energy intensity can vary abruptly with changes to the incident angle α. Multiple different angles were tested during this phase.

These angles were found and calculated with the help of Sébastien Popoff's script.

To facilitate the construction of the setup, a Python script was written to calculate the angle α_{1D}, the height of each post connected to the laser arm and the distance between the first post and the DMD (to avoid clipping the beam). This information is sufficient to achieve a coherent and correct setup.

Before starting to test the setup, the incident angle α had to be calculated. The Python script adapted from Sébastien Popoff's version generated multiple feasible solutions to evaluate. The first test, with $\alpha_1 = 32$ degrees, yielded unexpected results.

Wanting to verify the performance of the system, a new angle $\alpha_2 = 23.5$ degrees, was calculated with the goal of positioning the reflected beam correctly (along $\vec{n}$). A second test was run with this angle.

Consequently, further evaluation procedures were undertaken. In an effort to confirm that the initial test result was not a mere coincidence, we decided to reattempt the experiment using another angle ($\alpha_3 = 52$ degrees) provided by the program. The outcome turned out to be even more unfavorable than the initial one.

Finally, after making modifications to the system and the program, a suitable result was found during the fourth test using α_1.

8 Results and Discussion

The results of the tests were the following:

The first test was ran with an incident angle of $\alpha_1 = 32$ degrees. The results were unsatisfactory. While the energy efficiency was good, concentrated mostly into a single diffraction order, the position of the reflected beam was nowhere near the desired outcome, as shown in Fig.12.

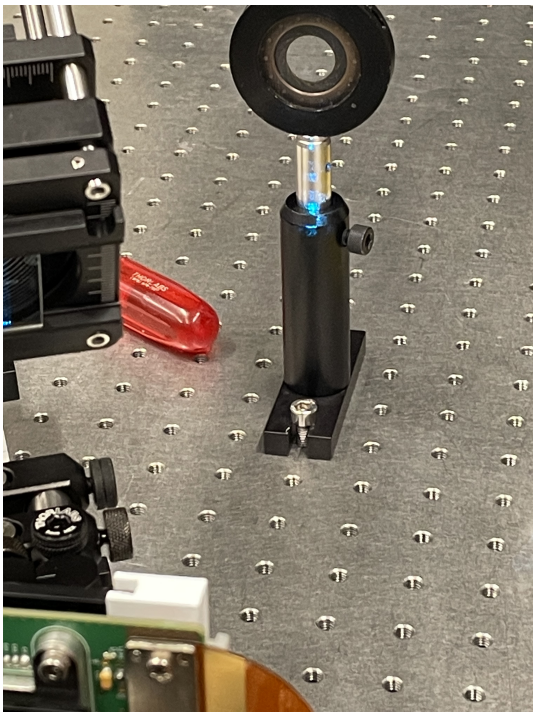

Figure 12: Results after the first test

Doubts about the performance of the setup began appearing, and in an effort to dispel any suspicion, the incident angle α_2 was calculated such that the orientation of the reflected beam, and the final position was good. Using the same equations as in section 2.4:

$$\beta_{1D} = 2\theta_{1D} - \alpha_{1D}$$

We can isolate α_{1D}:

$$\alpha_{1D} = 2\theta_{1D} - \beta_{1D}$$

Then transform the result into α_2:

$$\alpha_2 = \arctan\left(\frac{\tan\left(2\theta_{1D} - \beta_{1D}\right)}{\sqrt{2}}\right)$$

Where

$$\theta_{1D} = \arctan\left(\frac{\tan\left(\theta\right)}{\sqrt{2}}\right)$$

with $\theta = 12$ degrees or 0.20944 radians

Using these equations, the incident angle is found to be $\alpha_2 = 23.5$ degrees.

In this configuration, the reflected beam's orientation is correct. However, the intensity of the laser beam is split into multiple diffraction orders, as observed in Fig.13. This implies an immense loss of energy, as only a single copy will be used in the printing process. Nevertheless, the objective of this test, to verify the accurate performance of the system, was reached.

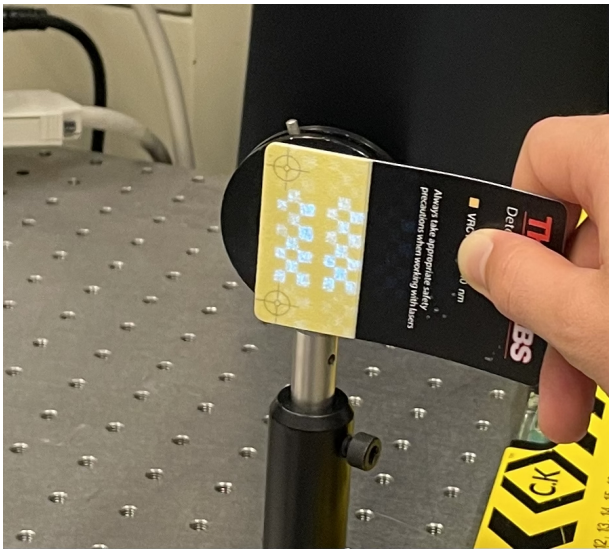

Figure 13: Results after the second test

Subsequently, another angle $\alpha_3 = 52$ degrees, calculated with the same script as α_1, was put to the test. The results were even more unfavorable. While the energy efficiency is still good, the positioning of the beam has gotten even worse, see Fig.14.

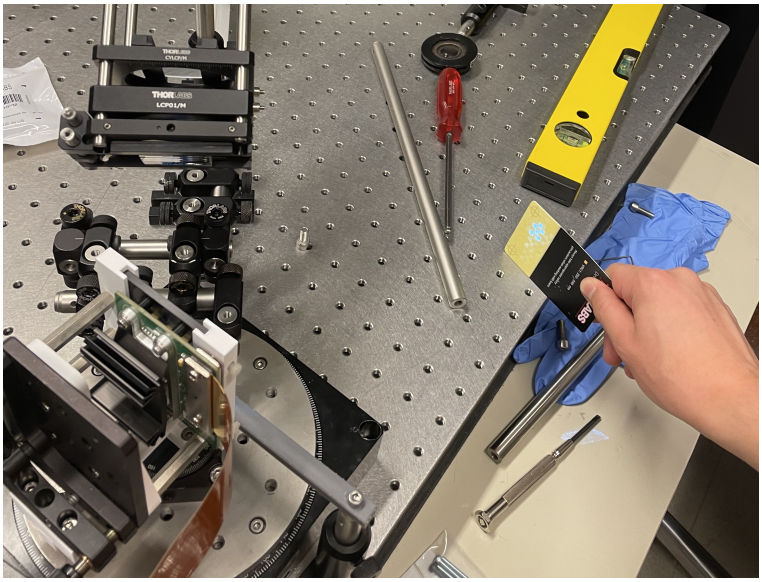

Figure 14: Results after the third test

The initial tests yielded inconclusive results, necessitating an inspection of the system's approach. Through a series of trial-and-error experiments and modifications of the setup, a viable solution appeared.

The modifications made to the support allow for a greater backwards rotation of the DMD (tilting it's screen up). The Python program was revised, taking into account the new movement of the system. This final solution shows a reflected beam oriented correctly, while having most of the light intensity focused into a single diffraction order, as exhibited in Fig.15.

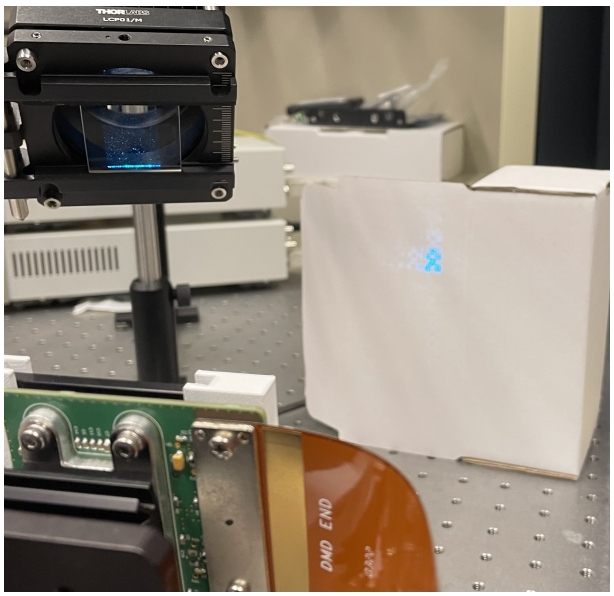

Figure 15: Results after the final test

9 Lessons learned

During this internship project, I gained valuable insights that will shape my future endeavors. Firstly, I realized the importance of meticulous planning and setting realistic goals. At times, I underestimated the complexity of certain tasks, which resulted in delays. Moving forward, I'll place a greater emphasis on project management and time allocation.

Challenges were an inevitable part of this journey. While setbacks were frustrating, they provided opportunities for growth. I learned to approach problems with resilience and creativity, often finding innovative solutions. These challenges also highlighted the significance of seeking help and guidance when necessary.

On a personal level, this internship allowed me to hone my independent work skills. I became adept at self-motivation, organization, and time management. I also realized the value of continuous learning and staying adaptable in the face of evolving tasks.

In retrospect, I believe that a more structured daily routine could have improved my efficiency. Additionally, seeking guidance earlier would have helped me overcome hurdles more swiftly.

These lessons learned will undoubtedly influence my future projects and career path. I'm committed to applying my newfound skills and knowledge to excel in future opportunities, and I'm excited to continue my journey of growth and development.

10 Conclusion

In this research project, I embarked on a journey to enhance the functionality and versatility of EPFL's LAPD's 3D printer, by developing a new support structure for the Digital Micromirror Device (DMD). The primary objective was to facilitate calibration and implement the utilization of lasers with varying wavelengths, all while accommodating the considerable needs of the equipment.

Throughout the project, I dove into the intricacies of tomographic volumetric 3D printing, a cutting-edge technology with the potential to reshape manufacturing and research landscapes. This technique, distinguished by its speed and precision, relies heavily on the correct alignment of optical components, notably the DMD.

The design phase introduced a transformative approach, built around the integration of two rotation stages, ensuring that the DMD remained stationary during adjustments. This new development addressed issues with the previous design, offering greater flexibility and precision in alignment.

The prototyping phase was instrumental in validating the design, highlighting potential stability concerns, which were duly addressed. The meticulous alignment of the laser arm, featuring multiple lenses, added another layer of complexity but was vital to achieving accurate results.

During the testing phase, I encountered challenges in optimizing diffraction efficiency while maintaining the correct beam orientation. A series of iterations and adjustments ultimately led to a solution that combined the best aspects of the experiments—correct beam orientation, minimal energy loss, and efficient diffraction.

This project offered valuable lessons in project management, problem-solving, and the importance of seeking guidance when faced with challenges. It also reinforced the significance of adaptability and a structured daily routine in research endeavors.

In conclusion, these efforts have resulted in a refined support structure that not only meets the original objectives but also paves the way for future advancements in tomographic volumetric 3D printing. We have demonstrated the feasibility of accommodating multiple laser wavelengths and optimizing diffraction efficiency. This project serves as a testament to the interdisciplinary nature of research, combining mechanical design, optics, and experimental precision.

As I conclude this chapter, I look forward to further exploration and refinement of this technology, knowing that my contributions have laid a foundation for future innovations in the field of applied photonics devices.

11 Acknowledgments

I would like to express my deepest gratitude to Professor Moser, my research lab professor, for his guidance and trust throughout my internship.

I am also grateful for the opportunities provided by EPFL and the Laboratory of Applied Photonics Devices, without whom, I wouldn't have been able to partake in this amazing adventure.

I am also indebted to Jorge Madrid Wolff, Maria Isabel Alvarez Castaño and Felix Wechsler for their valuable mentorship and collaboration, which greatly enriched my understanding of applied photonic devices and the

underlying theoretical principles.

The camaraderie and support of my fellow interns and lab colleagues were invaluable. I especially appreciate Jean Claude Rihani and Göktuğ İlter for their collaborative spirit and the knowledge-sharing environment they fostered in our shared office.

I would like to acknowledge the Laidlaw Foundation for their support, which made this internship possible.

I am grateful to my family and friends for their unwavering encouragement and understanding during this journey.

This internship experience has been transformative, and I am fortunate to have had the support of these individuals and organizations. Their contributions have not only shaped my research skills but have also inspired my future aspirations in engineering.

References

[1] D. Loterie, P. Delrot, and C. Moser, "High-resolution tomographic volumetric additive manufacturing," *Nature communications*, vol. 11, no. 1, p. 852, 2020.

[2] S. Popoff, "Setting up a dmd: Diffraction effects," https://www.wavefrontshaping.net/post/id/21#fig5, 2016, accessed: 10-07-2023.

[3] ——, "blazing_angle_dmd.ipynb," https://github.com/wavefrontshaping/WFS.net/blob/master/blazing_angle_DMD.ip 2016.

[4] N. Blondon, "dmdcalibration.py," https://github.com/nicoblon/dmdCalibration.py, 2023.

[5] M. Biselx, "Reflectance measure program," https://github.com/mbiselx/reflectance_measure/tree/main, 2023.